Consumption of Fluoroethylene Carbonate (FEC) on Si-C Composite Electrodes for Li-Ion Batteries

Roland Jung,[a,b,*,z] Michael Metzger,[a,*] Dominik Haering,[a,*] Sophie Solchenbach,[a,*] Cyril Marino,[a,c] Nikolaos Tsiouvaras,[b] Christoph Stinner,[b] and Hubert A. Gasteiger[a,]**

[a]*Chair of Technical Electrochemistry, Department of Chemistry and Catalysis Research Center, Technische Universität München, Garching, Germany*
[b]*BMW AG, Munich, Germany*

The electrolyte additive fluoroethylene carbonate (FEC) is known to significantly improve the lifetime of Li-ion batteries with silicon anodes. In this work, we show that FEC can indeed improve the lifetime of silicon-carbon composite anodes but is continuously consumed during electrochemical cycling. By the use of ^{19}F-NMR spectroscopy and charge/discharge cycling we demonstrate that FEC is only capable to stabilize the cell performance as long as FEC is still remaining in the cell. Its total consumption causes a significant increase of the cell polarization leading to a rapid capacity drop. We show with On-line Electrochemical Mass Spectrometry (OEMS) that the presence of FEC in the electrolyte prohibits the reduction of other electrolyte components almost entirely. Consequently, the cumulative irreversible capacity until the rapid capacity drop correlates linearly with the specific amount of FEC (in units of $\mu mol_{FEC}/mg_{electrode}$) in the cell. The latter quantity therefore determines the lifetime of silicon anodes rather than the concentration of FEC in the electrolyte. By correlating the cumulative irreversible capacity and the specific amount of FEC in the cell, we present an easy tool to predict how much cumulative irreversible capacity can be tolerated until all FEC will be consumed in either half-cells or full-cells. We further demonstrate that four electrons are consumed for the reduction of one FEC molecule and that one carbon dioxide molecule is released for every FEC molecule that is reduced. Using all information from this study and combining it with previous reports in literature, a new reductive decomposition mechanism for FEC is proposed yielding CO_2, LiF, Li_2O, Li_2CO_3, H_2 and a partially cross-linked polymer.
 [DOI: 10.1149/2.0951608jes]

Manuscript submitted March 11, 2016; revised manuscript received May 23, 2016. Published June 9, 2016.

In the emerging market of electric vehicles (EVs), the development of batteries with higher energy density and improved cycle-life is essential.[1] However, their penetration of the mass market significantly depends on cost and the available driving range.[2] The US Advanced Battery Consortium (USABC) defined the target value of 235 Wh/kg (at a C/3 rate) on a battery level until 2020.[3] As outlined in the recent review by Andre et al.,[4] reaching this goal requires an increase of the energy density of today's batteries by a factor of roughly 2 to 2.5 and can only be achieved by the development and integration of novel anode and cathode active materials. A critical element to reach this goal is the implementation of anode active materials with much higher specific capacity than currently used graphite anodes (372 mAh/g[1,5,6]), with silicon being considered as the most likely next generation anode material due to its high natural abundance and very high theoretical specific capacity of roughly 3600 mAh/g (corresponding to the $Li_{15}Si_4$ phase[7]).

The alloying of silicon with lithium is accompanied by large structural changes, resulting in a volume increase by 310% upon full lithiation.[5,7–11] These huge volumetric changes upon lithium insertion and extraction are responsible for the generally shorter cycle-life of silicon electrode materials compared to commonly used graphite anodes. On the one hand, the volume expansion leads to irreversible capacity loss due to SEI formation on newly created surfaces induced by volume expansion/contraction during charge/discharge, so that electrolyte is continuously consumed during cycling. On the other hand, the volumetric changes can cause particle cracking, resulting in the loss of electrical contact. By using nanostructured electrodes, the mechanical cracking of the particles causing loss of electrical contact can be avoided.[11–18] In particular, Liu et al. showed that silicon particles with a diameter of up to 150 nm can be lithiated without crack formation.[16] However, the surface area increases drastically when nanosized silicon is used and therefore the irreversible capacity loss caused by solid electrolyte interface (SEI) formation also rises. For example, Chan et al. used silicon nanowires which showed almost no capacity fading for the first ten cycles, but observed an irreversible capacity of around 27% in the first cycle.[12] Li et al. on the other hand used nanostructured silicon particles with a diameter of 78 nm and reported high capacities with comparably high areal loadings but at the same time high capacity fading from ≈2100 mAh/g_{Si} to ≈1730 mAh/g_{Si} within ten cycles.[19] Even though the particle cracking can be prevented, mathematical modeling suggests that the SEI formed on the silicon particles cracks during the volumetric changes, causing a continuous electrolyte consumption and loss of active lithium.[20,21] However, Etacheri et al. showed that substantial improvement can be achieved by using fluoroethylene carbonate (FEC) as electrolyte additive, which significantly reduces irreversible capacities and leads to improved cycling stability.[22] In particular, a reduction of the irreversible capacity by roughly 50% was observed when FEC was used in comparison to FEC-free electrolytes. Furthermore, comparing FEC-containing and FEC-free electrolytes, the capacity decay from cycle 2 to cycle 30 was drastically reduced from 80% to 30%.[22] This is consistent with the earlier report by Choi et al., who observed a capacity retention after 80 cycles of 89% with FEC additive in contrast to only 68% in FEC-free electrolyte.[23] Due to the significant improvement caused by FEC, it is nowadays established as a standard additive for silicon electrodes, even though the exact working principle and decomposition mechanism are not fully understood yet.[22–25]

In this study, we examine the effect and in particular the consumption of FEC on silicon-carbon composite electrodes. The continuous consumption of FEC is shown by ^{19}F-NMR spectroscopy and an observed sudden cell failure which is detected as a rapid drop in capacity is analyzed and related to the total consumption of FEC. It will be shown that FEC nearly suppresses the reduction of any other electrolyte component, which is consistent with the previous literature and suggests that the rate of FEC reduction is greater than the reduction of EC and linear carbonates.[26–31] Furthermore, due to the continuous consumption of FEC quantified by ^{19}F-NMR, the number of charge/discharge cycles over which silicon anodes can by stabilized by FEC is directly proportional to the total moles of FEC per

*Electrochemical Society Student Member.
**Electrochemical Society Fellow.
[c]Present address: Electrochemistry Laboratory, Paul Scherrer Institut, CH-5232 Villigen, Switzerland.
[z]E-mail: roland.jung@tum.de

gram of anode electrode, rather than the FEC concentration in the electrolyte. As a consequence, 10–20%$_{wt}$ FEC additive are highly effective when examined at the high electrolyte/active material weight ratios commonly used in small-scale test cells (e.g., coin cells), but are predicted to not provide long-term protection under the much lower electrolyte/active material weight ratios used in commercial cells. Combining our experimental observations with on-line electrochemical mass spectrometry (OEMS), it is possible to reveal that the reduction of FEC is an overall four-electron process, releasing one molecule of CO_2 per molecule of FEC; a new mechanism for the reductive decomposition of FEC is proposed.

Experimental

Electrode preparation.—The preparation of the binder lithium polyacrylate (LiPAA) was done in analogy to literature as a 10%$_{wt}$ solution in water,[32] diluting a 35%$_{wt}$ polyacrylic acid solution in water (PAA, $M_w \approx 250{,}000$ g/mol, from Sigma-Aldrich, Germany) with deionized water and neutralizing it with lithium hydroxide (LiOH, Sigma-Aldrich, Germany) to a pH-value of ≈8.

Electrodes were prepared with silicon particles (≈100 nm diameter, from Alfa Aesar, Germany), vapor grown carbon fibers (VGCF-H, from Showa Denko, Japan), and the above described LiPAA solution, setting a weight ratio of 40:40:20 Si/VGCF-H/LiPAA. The slurry was mixed with water in a planetary ball-mill (Pulverisette 7, from Fritsch, Germany) using zirconia balls with a diameter of 10 mm at 400 rpm for 3 × 15 minutes. For coin cell testing, the resulting ink was spread onto copper foil (thickness 12 μm, MTI Corporation, USA) using a gap bar coater (RK PrintCoat Instruments, UK). After drying at room temperature, electrodes with 10 mm diameter (0.79 cm^2 area) were punched, then dried overnight at 120°C under vacuum in a glass oven (drying oven 585, from Büchi, Switzerland), and subsequently transferred into a glove box without exposure to ambient air. The final loading of these electrodes used for half-cell testing in coin cells and Swagelok T-cells was 3.0 ± 0.6 mg$_{electrode}$/cm^2 (corresponding to a silicon loading of 1.2 ± 0.2 mg$_{Si}$/cm^2) and an electrode thickness of ≈50 μm. The theoretical areal capacity of these electrodes is thus 4.3 ± 0.9 mAh/cm^2 (≡1440 mAh/g$_{electrode}$) based on a theoretical capacity of 3600 mAh/g$_{Si}$[7] and neglecting the small capacity of the VGCF-H fibers (<80 mAh/g). For full-cell testing the loading of the Si electrode was 1.4 mg$_{electrode}$/cm^2 (0.6 mg$_{Si}$/cm^2, 2.1 mAh/cm^2). As counter electrode, a commercial LFP electrode with an areal capacity of 3.5 mAh/cm^2 (from Custom Cells, Itzehoe, Germany) was used.

The specific surface areas of electrode components were determined by BET, using an Autosorb iQ nitrogen gas sorption analyzer (Quantachrome Instruments, USA). The determined BET areas are 19 m^2/g for the silicon nanoparticles and 13 m^2/g for the VGCF-H fibers.

Electrochemical characterization.—Electrochemical cycling was performed in coin cells (Hohsen Corp., Japan) or Swagelok T-cells, assembled in an argon filled glove box (O_2 and H_2O < 0.1 ppm, from MBraun, Germany) using pure lithium (diameter of 15 mm in coin cells and 11 mm in Swagelok T-cells and thickness of 0.45 mm; battery grade foil, 99.9% purity, from Rockwood Lithium, USA) as anode, two glass fiber separators (glass microfiber filter #691, from VWR, Germany), and 75 or 150 μL LP57 electrolyte (1 M $LiPF_6$ in EC:EMC (3:7 wt/wt), <20 ppm H_2O, from BASF, Germany) to which different amounts of fluoroethylene carbonate (FEC, from Solvay, Belgium) were added. Additionally, for full-cell testing a cell was assembled using two H2013 separators (from Celgard, USA) and 30 μL LP57 electrolyte containing 2%$_{wt}$ FEC. As will be shown in the Results section, a critical variable is the molar amount of FEC normalized by the silicon electrode mass (in units of μmol$_{FEC}$/mg$_{electrode}$), thereafter referred to as specific amount of FEC, which is calculated from the added electrolyte volume, the electrolyte density (1.19 g/cm^3), the %$_{wt}$ of added FEC, and the molecular weight of FEC (106 g/mol).

In the case of Swagelok T-cells, a lithium reference electrode was used to monitor the potentials of working and counter electrode. The cells were cycled in a climate chamber (Binder, Germany) at 25°C with a battery cycler (Series 4000, from Maccor, USA) according to the following procedure: 3 cycles at a C-rate of C/10 and up to 450 cycles at C/3; the C-rate was referenced to the above described theoretical capacity of 4.3 ± 0.9 mAh/cm^2 (≡1440 mAh/g$_{electrode}$). The cells were cycled between 10 mV and 1.2 V vs. Li/Li$^+$ in constant current (CC) mode.

^{19}F-NMR.—After the cycling experiments, the coin cells were opened, the retrieved separators were soaked in 800 μL DMSO-d_6, and the resulting solution was filled into air-tight NMR tubes. The ^{19}F-NMR spectra were collected on a Bruker Ascend 400 (400 MHz) with and without proton decoupling. For the comparison of integral ratios only the non-decoupled spectra were used.

On-line electrochemical mass spectrometry (OEMS).—For OEMS experiments, it is necessary to use working electrodes coated on a porous substrate to allow for fast diffusion of evolved gases into the cell head space.[33] Coatings on aluminum or copper foil current collectors cannot be used, because the long diffusion time of gas produced at the working electrode to the head space of the cell would compromise the time and voltage resolution.[34] In this study, silicon electrodes were prepared by coating the above described ink onto carbon fiber paper (H2315, from Freudenberg, Germany). Since carbon fiber paper can also intercalate lithium, the overall electrode capacity is derived from the silicon capacity plus the capacity of the carbon fiber paper, which was determined to be roughly 190 mAh/g$_{C\text{-}paper}$. The working electrodes had a diameter of 15 mm (≡1.77 cm^2), with an areal weight of 1.04 mg/cm^2 for the Si/VGCF-H/LiPAA electrode and of 7.75 mg/cm^2 for the carbon fiber paper, corresponding to an overall areal capacity of 2.96 mAh/cm^2 (i.e., 1.50 mAh/cm^2 from the Si/VGCF-H/LiPAA electrode and 1.46 mAh/cm^2 from the carbon fiber paper). The surface area per cm^2 of electrode (Si + VGCF-H + C-paper) was determined by multiplying the areal masses of each component with its BET surface area. The measured BET surface area of the C-fiber paper was 0.5 m^2/g$_{C\text{-}paper}$ and with the surface areas of Si and VGCF-H (see above), the total surface area of the electrode was calculated to be 0.017 m^2/cm$^2_{electrode}$.

As counter electrode, a commercial LFP electrode with an areal capacity of 3.5 mAh/cm^2 (from Custom Cells, Itzehoe, Germany) and a diameter of 16 mm was used. Both electrodes were dried overnight at 120°C under vacuum in a glass oven (drying oven 585, from Büchi, Switzerland).

The OEMS cell was assembled in a glove box with argon atmosphere (O_2 and H_2O < 0.1 ppm, MBraun, Germany), using two glass fiber separators (glass microfiber filter #691, from VWR, Germany) and 320 μL LP57 electrolyte (1 M $LiPF_6$ in EC:EMC (3:7 wt/wt), <20 ppm H_2O, BASF, Germany) with added 5%$_{wt}$ FEC (Solvay, Belgium). The cell was placed in a climate chamber at 25°C (Binder, Germany) and connected to the potentiostat (Series G300 potentiostat, Gamry, USA) and the mass spectrometry system, which was described in detail elsewhere.[34] The cell was held at OCV for 3 h, followed by a galvanostatic charge from OCV (open circuit voltage) to 3.44 V with a current of 148 μA/cm^2, corresponding to a C-rate of C/20. The gas evolution during the OCV and the charging period was recorded by OEMS. All mass signals were normalized to the ion current of the ^{36}Ar isotope to correct for fluctuations of pressure and temperature. Conversion of the ion currents to concentrations was done for the CO_2, H_2 and C_2H_4 using a calibration gas (Ar with 2000 ppm H_2, O_2, C_2H_4 and CO_2, Westfalen, Germany). The total moles of each gas can then be determined from the OEMS cell volume (9.5 mL) and the ideal gas law.

Results

Electrochemical cycling of Si-based anodes.—Figs. 1 and 2 display the coulombic efficiency and specific lithiation capacity vs. cycle number for Si-Li coin cells with 75 μL (Fig. 1) or 150 μL (Fig. 2) of electrolyte. All cells contained an electrolyte based on 1 M $LiPF_6$

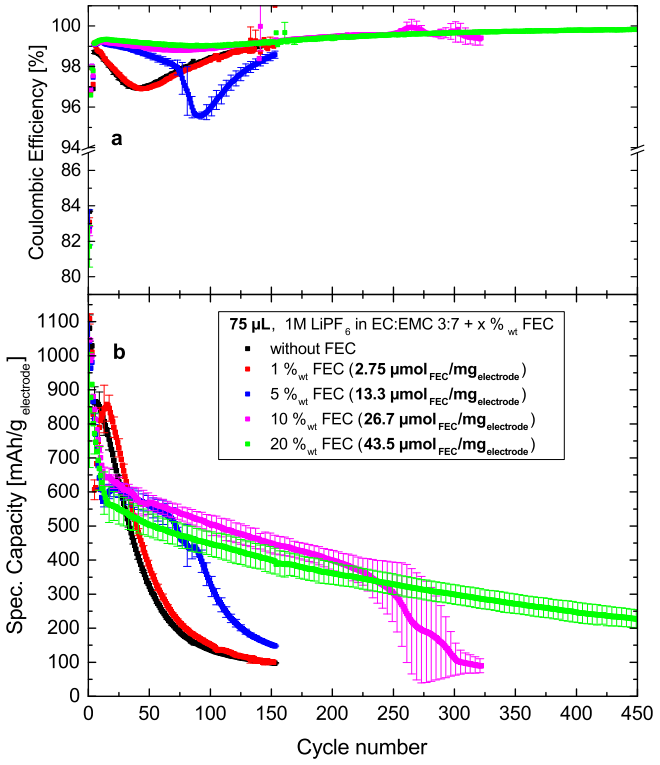

Figure 1. (a) Coulombic efficiency and (b) specific lithiation capacity vs. cycle number of Si-Li coin cells with 75 µL LP57 electrolyte containing different amounts of FEC. The first three cycles are conducted at C/10 followed by cycling at C/3. The theoretical capacity is 1440 mAh/$g_{electrode}$ and the specific amount of FEC (in $\mu mol_{FEC}/mg_{electrode}$) is specified in the figure.

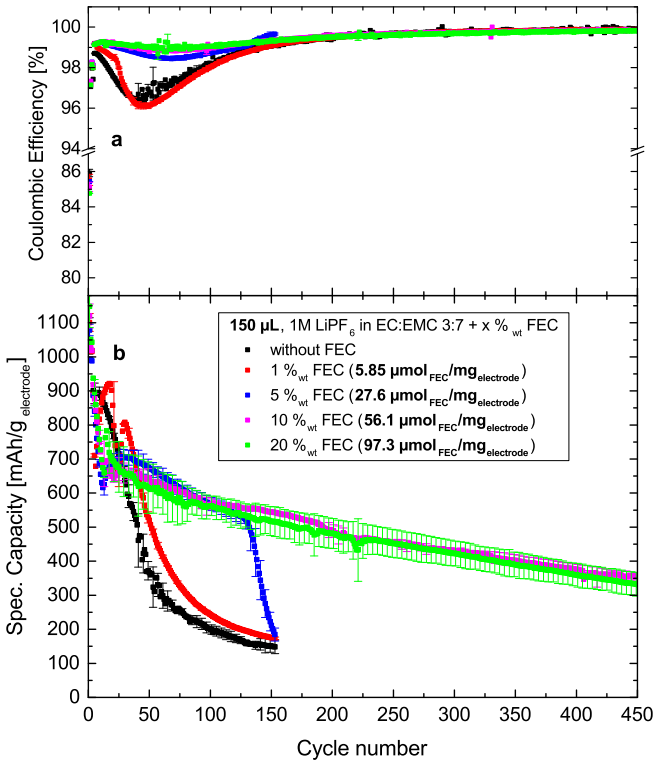

Figure 2. (a) Coulombic efficiency and (b) specific lithiation capacity vs. cycle number of Si-Li coin cells with 150 µL LP57 electrolyte containing different amounts of FEC. The first three cycles are conducted at C/10 followed by cycling at C/3. The theoretical capacity is 1440 mAh/$g_{electrode}$ and the specific amount of FEC (in $\mu mol_{FEC}/mg_{electrode}$) is specified in the figure.

in EC:EMC (3:7 wt/wt) with different levels of FEC (0, 1%$_{wt}$, 5%$_{wt}$, 10%$_{wt}$ and 20%$_{wt}$), and two cells were tested for each electrolyte composition. Two different volumes of electrolytes were selected in order to compare systems with equal concentrations but different amounts of FEC, thereby examining whether it is the concentration or the total moles of FEC which controls the lifetime of silicon based electrodes. Therefore, both the %$_{wt}$ of FEC as well as its molar amount referenced to the electrode mass (in units of $\mu mol_{FEC}/mg_{electrode}$) are specified in Figs. 1 and 2. The cells were cycled between 10 mV and 1.2 V vs. Li/Li^+ in constant current (CC) mode (first three cycles at C/10, followed by cycling at C/3). No constant voltage (CV) period was applied due to two reasons: i) it is reported in the literature that at voltages below 50 mV $Li_{15}Si_4$ starts to crystallize,[7] which is suspected to be very reactive and thus to diminish the lifetime of silicon electrodes;[35] ii) it significantly increases the sensitivity of electrochemical cells to changes in the polarization, since the CV phase would deliver additional capacity due to a shrinking polarization caused by a decreasing current.

The specific lithiation capacities in the third cycle at C/10 range from 915 to 1043 mAh/$g_{electrode}$ for all experiments shown in Figs. 1 and 2, equating to 63–73% of the theoretical capacity of 1440 mAh/$g_{electrode}$ (see Experimental section). For the cells containing 75 µL electrolyte (Fig. 1), two different trends can be observed. Firstly, the cells containing 0 and 1%$_{wt}$ FEC have a relatively poor coulombic efficiency and their specific capacities fade very rapidly from the very beginning, dropping to 150 mAh/$g_{electrode}$ after only 100 cycles (red and black symbols in Fig. 1). In contrast, cells containing $\geq$5%$_{wt}$ FEC show substantially improved coulombic efficiency and a fast decrease in specific capacity until cycle 15, which is likely due to the formation of an initially more resistive SEI with FEC, as was suggested before.[36] After this initially fast capacity loss, the capacity fading in the presence of FEC is much less than in electrolytes with <5%$_{wt}$ FEC. However, this trend is interrupted when a rapid capacity drop is observed at roughly cycle 70 for 5%$_{wt}$ FEC and at roughly cycle 225 for 10%$_{wt}$ FEC. The reason for the large error bars around the cycle numbers where the rapid capacity drop is observed is caused by the small offset between cycle numbers where the capacity drops occur in the two nominally identical cells. Interestingly, for the cells with 5%$_{wt}$ FEC, the rapid capacity drop is accompanied by a drop in the coulombic efficiency, indicating significant changes in the parasitic reactions related to SEI formation on silicon. This is not observed for the cells with 10%$_{wt}$ FEC, which might be due to the already very thick SEI after $\approx$200 cycles, in which case the disappearance of FEC (see below) has a less drastic effect. On the other hand, the cells containing 20%$_{wt}$ FEC do not display this rapid capacity drop until the end of the cycling test after 450 cycles. The cells with 150 µL electrolyte (Fig. 2) show the same overall behavior, except that the rapid capacity drop for the cells with 5%$_{wt}$ FEC now occurs at a higher cycle number (roughly cycle 130) and that it is not observed anymore for the cells with 10%$_{wt}$ FEC up to 450 cycles. However, for the cells containing 1%$_{wt}$ FEC the rapid capacity drop can be seen around cycle 25 (not observed with 75 µL FEC in Fig. 1) along with a simultaneous drop in coulombic efficiency. Remarkably, in analogy to the case for 10%$_{wt}$ FEC and 75 µL electrolyte (Fig. 1), for 150 µL the drop in coulombic efficiency after the rapid capacity drop is not observed for 5%$_{wt}$ FEC. A comparison of the data with 75 and 150 µL electrolyte (see Figs. 1 and 2) reveals that an increase of the specific amount of FEC ($\mu mol_{FEC}/mg_{electrode}$) is responsible for enhanced cycle life, rather than simply the concentration (%$_{wt}$) of FEC. This in turn suggests that the consumption of FEC might be the reason for the observed capacity drop. The correlation between FEC content and the onset of the rapid capacity drop is subject to the Discussion section.

Another interesting observation is that cells with FEC-free electrolyte have higher absolute capacities for the first 30–40 cycles. A very similar behavior was observed by Schroder et al., who reported higher capacities for FEC-free electrolytes until cycle 37, with similarly high fading rates.[36] This feature was explained by assuming that a sufficiently thick and stable SEI is formed in the presence of

FEC from the very beginning, whereas the SEI in FEC-free electrolyte might initially be thinner, causing less polarization and higher capacities, but at the same time is not stable enough for long term cycling.

NMR analysis of electrolyte before and after the capacity drop.— In order to understand the reason for the rapid capacity drop, we analyzed the electrolyte before and after the drop by ^{19}F-NMR spectroscopy to quantify the amount of remaining FEC in the cells. Fig. 3a shows three cells which were cycled in LP57 with 5%$_{wt}$ FEC. The cell shown in green (cell Si-Li #3) was stopped seven cycles after the clearly visible onset of the rapid capacity drop after roughly 120 cycles. This is somewhat larger than what was observed for the nominally identical experiment shown in Fig. 1 (blue line, with also 75 µL electrolyte and 5%$_{wt}$ FEC), which is due to the slightly higher specific amount of FEC used in Fig. 3a (15.7 µmol$_{FEC}$/mg$_{electrode}$ for the green line) compared to what was used in Fig. 1 (13.3 µmol$_{FEC}$/mg$_{electrode}$); the quantitative relationship between the specific amount of FEC and the cycle number at which the rapid capacity drop is observed will be shown in the Discussion section. The cells plotted in black (cell Si-Li #1) and red (cell Si-Li #2) were stopped when roughly one third

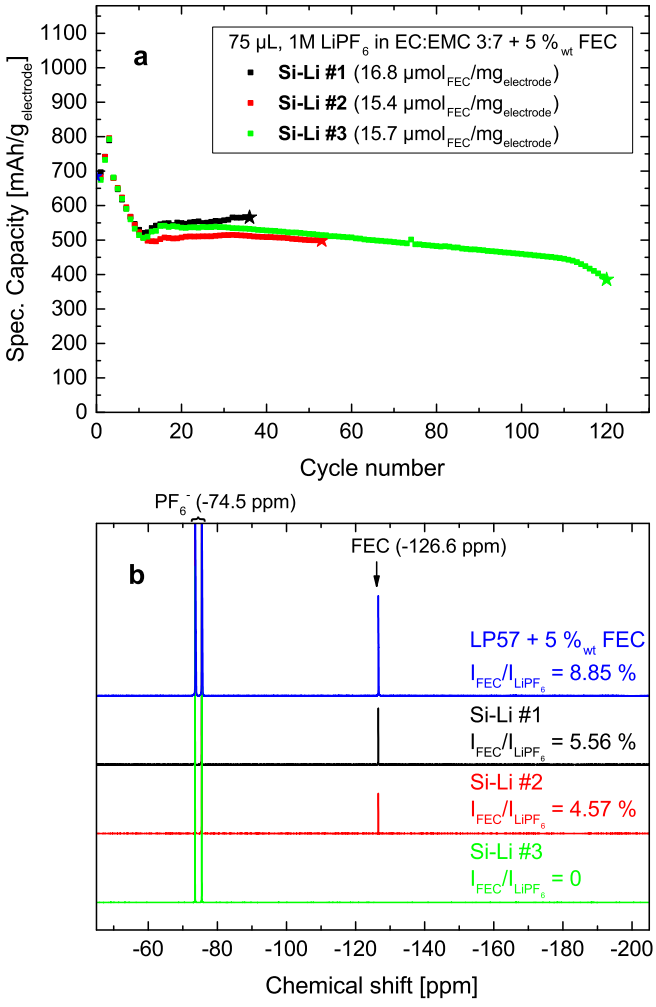

Figure 3. (a) Specific lithiation capacity vs. cycle number of Si-Li coin cells (Si-Li #1 = black line; Si-Li #2 = red line; Si-Li #3 = green line) with 75 µL LP57 electrolyte containing 5%$_{wt}$ FEC (the moles of FEC per mg$_{electrode}$ is specified in the figure); cycling rates are C/10 for the first 3 cycles and C/3 for all subsequent cycles. (b) ^{1}H-decoupled ^{19}F-NMR-spectra of the electrolyte before cycling (blue) and after cycling of the three cells shown in (a); the intensity ratios between the fluoride signal from FEC and from $LiPF_6$ (I_{FEC}/I_{LiPF6}) is given in the figure and were calculated from the non-decoupled spectra.

and one half of the FEC were expected to be consumed, respectively (i.e., after cycle 36 and 53). For all the cells, the electrolytes were extracted and liquid state ^{19}F-NMR spectra were measured (Fig. 3b). Since the decomposition of $LiPF_6$ in comparison to the solvent is expected to be negligible, $LiPF_6$ was used as an internal standard to quantify the amount of remaining FEC, namely by determining the integral ratio of the fluorine signal from FEC and that of $LiPF_6$; note that the integral ratio of the electrolyte before cycling (blue spectrum in Fig. 3b) fits exactly the expected ratio of FEC:$LiPF_6$ in pure LP57 + 5%$_{wt}$ FEC. The assumption that the $LiPF_6$ concentration does not change significantly over the course of the experiments is supported by a detailed inspection of the NMR-spectra, revealing no additional peaks from salt decomposition products like $PO_2F_2^-$. Additionally, no signals originating from SiF_6^{2-} (typically observed product in the event of glass fiber separator decomposition by HF)[37] were observed in the ^{19}F-NMR experiments, proving that the glass fiber separator is stable under our experimental conditions.

When comparing the integral ratios of FEC and $LiPF_6$ in Fig. 3b, a steady decrease of the FEC concentration with increasing cycle number can be observed. While 63% of FEC is still left in the cell after cycle 36 (from $(I_{FEC}/I_{LiPF6})_{36\ cycles}$ / $(I_{FEC}/I_{LiPF6})_{0\ cycles}$; see black lines/numbers in Fig. 3), the remaining amount of FEC has dropped to 52% after 53 cycles (see red lines/numbers in Fig. 3). For the Si-Li cell which was opened after the capacity drop at cycle 120, the remaining FEC concentration based on the ^{19}F NMR data is zero (see green lines/numbers in Fig. 3). This provides clear evidence for the continuous consumption of FEC during charge/discharge cycling of silicon based anodes, consistent with the proposed cracking of the SEI upon volume expansion.[20,21] Extension of this NMR analysis further suggests that the rapid capacity drops observed in Figs. 1 and 2 occur at the point once the FEC additive is consumed. This explains why the rapid capacity drop appears at higher cycle numbers when the specific amount of FEC (i.e., the µmol$_{FEC}$/mg$_{electrode}$) is increased, as can be observed by comparing Figs. 1 and 2. A more detailed quantitative correlation will be provided in the Discussion section.

Analysis of cell polarization by three electrode setup.— A three electrode set-up with lithium reference electrode (Swagelok T-cells) is used to separately analyze the voltage evolution of the silicon working electrode and the lithium counter electrode in order to determine the polarization of the silicon electrode over the course of the charge/discharge cycles. Figs. 4a and 4b show the cycle number dependence of the Si-Li cell capacity and the evolution of the mean charge/discharge voltage polarization ΔV_{mean} for each electrode, whereby ΔV_{mean} is the difference between $\int(V_{delith.} \cdot dq_{delith.})/\int dq_{delith.}$ and $\int(V_{lith.} \cdot dq_{lith.})/\int dq_{lith.}$ evaluated for each charge/discharge cycle with voltages referenced to the potential of the lithium reference electrode. The cycle number at which the rapid capacity drop occurs as well as its correlation to the specific amount of FEC is more difficult to predict in these measurements in Swagelok T-cells, since contrarily to coin cells, the exact amount of available electrolyte in a Swagelok T-cell cannot be determined reliably.

It can be seen that the polarization of the lithium counter electrode changes very little when the capacity starts to fade more rapidly (see red line in Fig. 4b), indicating that lithium is not much affected by the consumption of FEC. In contrast, the polarization of the silicon electrode increases significantly (see black line in Fig. 4b) from roughly 300 mV to over 400 mV once FEC is consumed. This significant rise of the silicon overpotential is probably the reason for the rapid capacity drop near cycle 40. This effect can be also seen in the cell-voltage profiles of the 30th (before the rapid capacity drop) and 50th cycle (after the rapid capacity drop) shown in Fig. 4c. An increase of the mean cell polarization from around 266 mV to 365 mV is observed. As the lithiation potential profile has a very flat slope, this higher polarization leads to a significantly lower lithiation capacity at the point at which the lower cutoff voltage is reached and consequently causes the rapid drop in capacity.

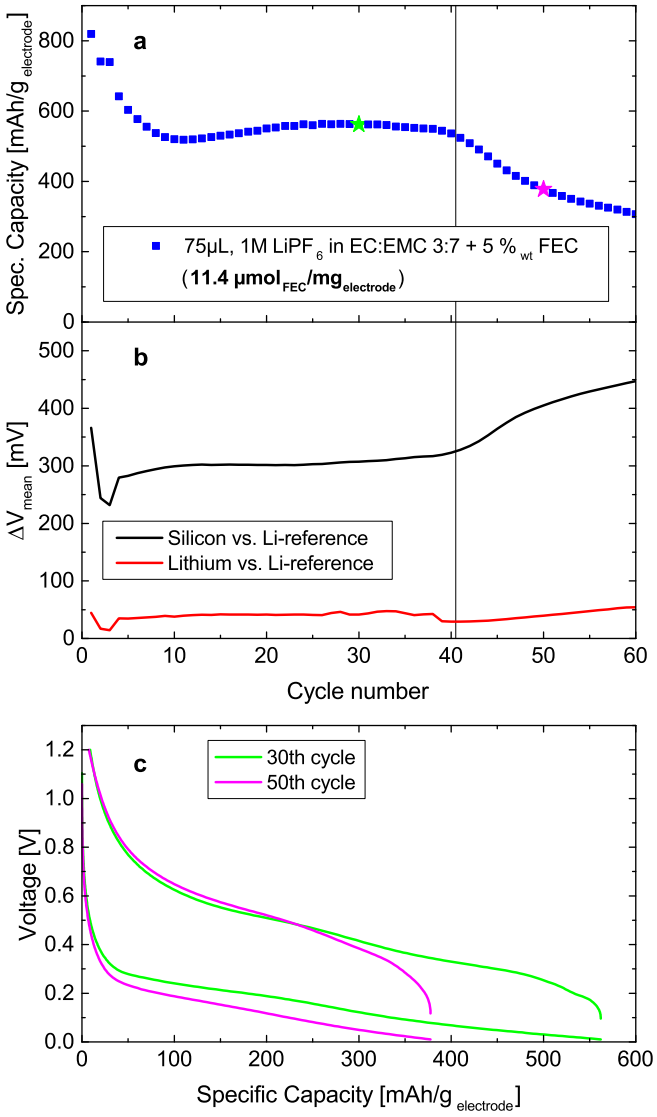

Figure 4. (a) Specific lithiation capacity vs. cycle number of a Si-Li Swagelok T-cell with a metallic lithium reference electrode using 75 µL LP57 electrolyte containing 5%$_{wt}$ FEC at a C-rate of C/10 for the first three cycles followed by cycles at C/3. (b) Mean charge/discharge voltage ΔV_{mean} (see definition in the text) vs. cycle number of both the silicon and lithium electrode with respect to the lithium reference electrode potential. (c) Cell voltage profile of the 30th cycle (i.e., before the rapid capacity drop) and the 50th cycle (i.e., after the rapid capacity drop) of the cell shown in (a).

Gas analysis of Si-LFP cell by OEMS.—The results of the online electrochemical mass spectrometry (OEMS) measurement of a Si-LFP cell during silicon lithiation are shown in Fig. 5. In the upper panel (Fig. 5a), the cell voltage profile during lithiation is shown by the black line, while the red line gives the potential of the silicon electrode vs. the Li/Li^+ potential calculated from the known LFP potential of ≈3.45 V. The use of LFP instead of Li metal will prevent the decomposition of the electrolyte on the counter electrode, since the electrolyte is stable at the potential of the LFP electrode so that all evolved gases can be traced back to reactions occurring on the silicon working electrode. In the lower panel (Fig. 5b), the mass traces of carbon dioxide (black), hydrogen (red) and ethylene (blue) are shown in terms of ppm in the cell head space and in terms of µmol/m$^2_{electrode}$; note that the surface area is the sum of the surface areas of silicon, VGCF-H, and the C-fiber paper (see Experimental section). It is known that EC reduction leads to ethylene evolution,[38–40] whereas FEC reduction causes carbon dioxide evolution,[41] analogous to the CO_2 evolution observed during the reduction of chloroethylene

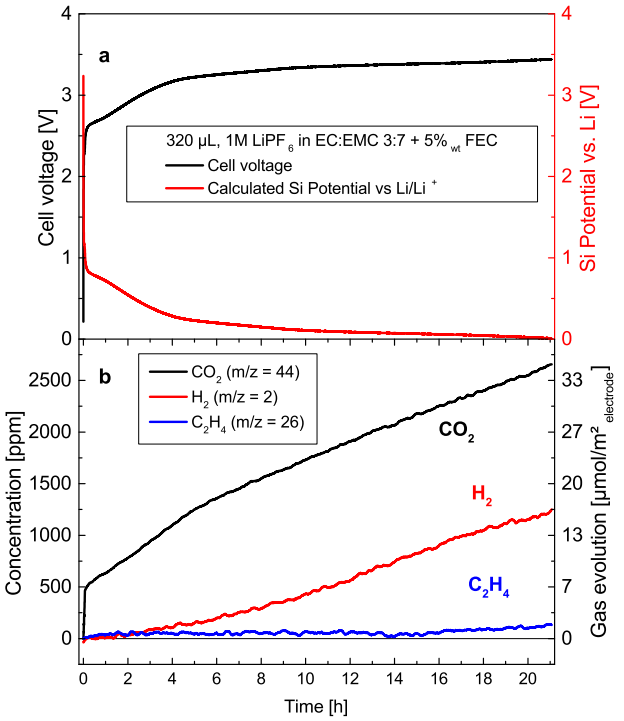

Figure 5. (a) Cell-voltage (black) and calculated silicon potential (red) vs. time of a cell using a silicon working electrode coated on carbon paper vs. a LFP counter electrode with 320 µl electrolyte (1 M $LiPF_6$ in EC:EMC (3:7 wt/wt) + 5%$_{wt}$ FEC), galvanostatically charged with a rate of C/20 from OCV to 3.44 V. (b) Evolution of CO_2 (black), H_2 (red) and C_2H_4 (blue) as a function of time. The OEMS data are smoothed, baseline corrected, and converted into units of [ppm] and [µmol/m$^2_{electrode}$]. The latter is calculated by converting the ppm into µmol and normalizing it to the surface area of Si + VGCF-H + C-fiber paper. The specific amount of FEC referenced to the Si/VGCF-H/LiPAA electrode is 91.8 µmol$_{FEC}$/mg$_{electrode}$.

carbonate.[42] Therefore, a quantification of these two gases gives information on the ratio of decomposed FEC and EC. The observed gas evolution (Fig. 5b) shows 2700 ppm of carbon dioxide, whereas the ethylene concentration amounts to only ≈100 ppm at the end of the lithiation process. That the latter is strikingly low can be seen by comparing it with the ≈2000 ppm C_2H_4 which were observed during the first lithiation of a graphite electrode with comparable areal capacity (2.5 mAh/cm^2) in the same electrolyte without FEC additive.[43] This, together with the fact that the molar ratio of evolved CO_2 to C_2H_4 at the end of the measurement is very large ($n_{CO2}/n_{C2H4} \approx 95:5$) clearly proves that FEC almost entirely suppresses the reduction of EC. Hence, one can assume that FEC is exclusively reduced as long as there is FEC present in the electrolyte. This fits well with the earlier observation that the interfacial resistance and thus the SEI changes significantly once the FEC is consumed (see Fig. 4).

In the evolution of CO_2, three regions with different rates (i.e., different slopes in Fig. 5b) can be observed. One with very high CO_2 evolution rate at the very beginning, where 460 ppm CO_2 are formed within the first 4.2 minutes of the measurement. A second region with a lower and constant rate until roughly five hours into the charging process, and a third region with a yet lower CO_2 evolution rate lasting until the end of the measurement. In contrast, the evolution of hydrogen does not start until about 2–3 hours after the start of the charging process and then proceeds with a more or less constant rate. During the entire measurement, no carbon monoxide was detected. Also, no SiF_4 (typical product upon HF attack on glass fiber separator)[44] was observed in the OEMS measurement, proving once again the stability of the separator under our experimental conditions. A more detailed analysis including the interpretation of these observations will be subject of the Discussion section.

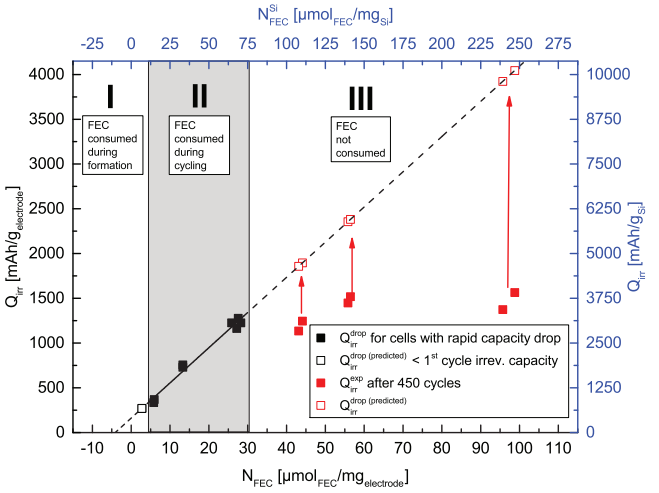

Figure 6. Cumulative irreversible capacity Q_{irr}, (see Equation 1) vs. specific amount of FEC in the cell (N_{FEC}) obtained from the cycling data shown in Figs. 1 and 2. Black squares: cells for which a rapid capacity drop was observed during cycling; full red squares: cells which did not show a rapid capacity drop until the end of the cycling experiment (450 cycles); open red squares: predicted Q_{irr} ($\equiv Q_{irr}^{drop\ (predicted)}$) by which one would expect to observe a rapid capacity drop; open black square: cells for which the specific amount of FEC was too low to obtain improved cycle life (i.e., all FEC gets consumed in the first formation cycle). The black line is a least-squares regression line through the data obtained for the 8 cells which showed a rapid capacity drop (black squares): $Q_{irr}^{drop\ (predicted)} = 39.3\ (mAh/g_{electrode})/(\mu mol_{FEC}/mg_{electrode}) \times N_{FEC} + 162\ mAh/g_{electrode}$ ($R^2 = 0.978$), with an x-axis intercept of 4.1 $\mu mol_{FEC}/mg_{electrode}$. Additionally, Q_{irr} and the specific amount of FEC normalized to the mass of silicon (N_{FEC}^{Si}) are shown in blue (right and top axes, respectively); normalized to silicon, the black regression line is: $Q_{irr}^{drop\ (predicted)} = 39.3\ (mAh/g_{Si})/(\mu mol_{FEC}/mg_{Si}) \times N_{FEC}^{Si} + 405\ mAh/g_{Si}$.

Discussion

Correlation between the cumulative irreversible capacity and FEC consumption.—The pronounced difference in cycling stability between the cells with and without FEC (Figs. 1 and 2) suggests that the SEI formed with FEC is significantly more stable. It is very interesting that independent of the amount of FEC, the cycling stability is nearly equal for all the cells as long as FEC is present in the electrolyte. This is due to the almost exclusive SEI formation by FEC, since its decomposition is preferred over that of EC and other electrolyte components, suppressing their decomposition to a very minimum. This is in accordance with the findings by Wang et al., who did not observe any EC reduction peak in a cyclic voltammetry experiment once FEC was present in the electrolyte.[31] Assuming therefore that all irreversible capacity is caused exclusively by FEC reduction, the lifetime of the cells should correlate with the irreversible capacity. In order to prove this for all cells with an observable rapid capacity drop (Fig. 1 and 2), the cumulative irreversible capacity, Q_{irr}, was calculated according to Equation 1, with $Q_i^{lithiation}$ and $Q_i^{delithiation}$ being the specific lithiation and delithiation capacity of the i^{th} cycle, summed up from the first cycle i = 1 until either the cycle where the rapid capacity drop occurs or to the end of the experiment (450 cycles):

$$Q_{irr} = \sum_i \left(Q_i^{lithiation} - Q_i^{delithiation}\right) \quad [1]$$

The calculated value of Q_{irr} for all the cells is plotted in Fig. 6 versus their respective specific amount of FEC, N_{FEC}. The full black squares represent the cells for which a rapid capacity drop was observed during the cycling experiment, yielding $Q_{irr} \equiv Q_{irr}^{drop}$. With increasing specific amounts of FEC in the cells, Q_{irr}^{drop} increases linearly (see black symbols in Fig. 6), representing the longer lifetime of cells with higher specific amount of FEC. If the reduction of FEC would be only one among several side reactions, one would not expect the clearly linear trend of Q_{irr}^{drop} vs. N_{FEC}, which in turn strongly supports the hypothesis that there is only one source of irreversible capacity, namely the reduction of FEC. The intercept of the linear correlation line with the y-axis (i.e., at $N_{FEC} = 0$) can be interpreted as the irreversible capacity of the first cycle (formation cycle) equating to 162 $mAh/g_{electrode}$. On the other hand, the x-axis intercept (i.e., at $Q_{irr} = 0$) represents the specific amount of FEC consumed during the first formation cycle, viz., 4.1 $\mu mol_{FEC}/mg_{electrode}$. Alternatively, the latter can also be interpreted as the minimum amount of FEC necessary in a cell to improve its cyclability.

Table I. Specific amount of FEC (N_{FEC}) and experimentally observed cumulative irreversible capacity (Q_{irr}^{exp}) for cells for which no rapid capacity drop was observed, either because all FEC was already consumed in the first cycle (rows 1 and 2) or because the total number of cycles in the experiment (450 cycles) was too low to lead to rapid capacity loss, i.e., too low to consume all the FEC (rows 3-8). For the latter, the predicted cumulative irreversible capacity at which one would expect the rapid capacity drop ($Q_{irr}^{drop\ (predicted)}$) obtained from the linear regression line in Fig. 6 is also given. The data are extracted from the experiments shown in Figs. 1 and 2.

Cell details	N_{FEC} [$\mu mol_{FEC}/mg$]	Q_{irr}^{exp} [mAh/g]	$Q_{irr}^{drop\ (predicted)}$ [mAh/g]
1% FEC, 75 µL	2.73	-	-
1% FEC, 75 µL	2.78	-	-
20% FEC, 75 µL	43.13	1135	1860
20% FEC, 75 µL	44.10	1245	1898
10% FEC, 150 µL	55.82	1448	2361
10% FEC, 150 µL	56.45	1518	2386
20% FEC, 150 µL	95.69	1374	3939
20% FEC, 150 µL	98.77	1565	4061

This model is well suited to predict at which cumulative irreversible capacity values cells with a defined specific amount of FEC, N_{FEC}, start to experience a rapid capacity drop due to the total consumption of FEC. The open question, however, is why for some cells the rapid capacity drop was not observed during the cycling experiments. To address this question, the cumulative irreversible capacity up to 450 cycles (Q_{irr}^{exp}) of the cells which did not exhibit a rapid capacity drop are plotted vs. N_{FEC} in Fig. 6 (full red squares). After 450 cycles (i.e., after the end of the experiment), the Q_{irr}^{exp}-values of these cells clearly lie below the Q_{irr}^{drop}-values predicted by the linear correlation line in Fig. 6, $Q_{irr}^{drop\ (predicted)}$ (see open red squares in Fig. 6), which suggests that the FEC additive had not been consumed at this point. For these cells, the values of N_{FEC}, Q_{irr}^{exp}, and $Q_{irr}^{drop\ (predicted)}$ obtained from the regression line equation (see caption of Fig. 6) are listed in Table I. The two cells with 1%$_{wt}$ FEC and 75 µL electrolyte (first two rows in Table I and open black squares in Fig. 6) contain only 2.73 and 2.78 $\mu mol_{FEC}/mg_{electrode}$, which is below the 4.1 $\mu mol_{FEC}/mg_{electrode}$ consumed during formation and is thus consistent with the fact that no improved lifetime was observed.

In order to make this model more generally applicable to other silicon based electrodes, the top x-axis and right y-axis in Fig. 6 (blue axes) were re-scaled to show the specific amount of FEC and the cumulative irreversible capacity normalized to the mass of silicon. This depiction is very useful under the assumption that all irreversible capacity stems from side reactions on silicon (expected to be the case after the first cycle for any silicon-carbon composite electrode), in which case the equation correlating Q_{irr} and N_{FEC}^{Si} (given in the caption of Fig. 6) can serve as an easy tool to calculate from a known specific amount of FEC how much irreversible capacity can be accumulated until all FEC is consumed. Only if one uses electrodes with low silicon and high graphite content, one would need to correct the y-axis intercept by the SEI formed on graphite. The slope, however, would stay constant since even for these electrodes, the irreversible

Table II. Comparison of the remaining amount of FEC after the cycling of various cells with either 2 or 5%$_{wt}$ FEC in LP57 electrolyte. The remaining FEC content was calculated from Q_{irr}^{exp} and $Q_{irr}^{drop\ (predicted)}$ using Equation 2 ($FEC_{rem.\ (EC)}$) or from the changes of the integral ratio of the FEC and the $LiPF_6$ peak in the NMR-spectrum ($FEC_{rem.\ (NMR)}$). Three different cell types were tested/evaluated: a) the data for the cells Si-Li #1-3 are taken from Fig. 3; b) the Li-Li cells were cycled at the same current over the same time as the Si-Li #1 cell, passing the same amount of total coulombs (the data in the table represent the average of three independent experiments); c) the Si-LFP cells consisted of a silicon-carbon composite anode with a lower loading and a commercial LFP electrode (see Experimental) which were cycled by the same procedure as that used for the Si-Li #1-3 cells (i.e., cycling at C/10 for the first 3 cycles and C/3 for all subsequent cycles). Si-LFP #1 was cycled with glass fiber and Si-LFP #2 with Celgard H2013 separators.

		Electrochemical data				NMR data	
Electrolyte		N_{FEC} [μmol/mg]	Q_{irr}^{exp} [mAh/g]	$Q_{irr}^{drop\ (predicted)}$ [mAh/g]	$FEC_{rem.\ (EC)}$ [%]	$\frac{I_{FEC}}{I_{LiPF_6}}$ [%]	$FEC_{rem.\ (NMR)}$ [%]
75 μL LP57 + 5%$_{wt}$ FEC	Electrolyte	-	-	-	**100**	8.85	**100**
	Si-Li #1	16.80	313	822	**62**	5.56	**63**
	Li-Li cell	-	-	-	**-**	5.62	**63**
	Si-Li #2	15.45	380	769	**51**	4.57	**52**
	Si-Li #3	15.73	880	780	**0**	0	**0**
75 μL LP57 + 2%$_{wt}$ FEC	Electrolyte	-	-	-	**100**	3.75	**100**
	Si-LFP #1	14.80	776	1488 (see text)	**48**	1.76	**47**
30 μL LP57 + 2%$_{wt}$ FEC	Electrolyte	-	-	-	**100**	3.29	**100**
	Si-LFP #2	5.45	482	752 (see text)	**36**	1.07	**33**

side reactions after the first cycle will be dominated by reactions occurring on silicon.

To validate our above interpretation of the linear regression model, viz., that it describes the point at which FEC will be consumed, we will do a more detailed analysis of the ^{19}F-NMR data shown in Fig. 3. As discussed before, no decomposition products of $LiPF_6$ are observed by NMR (Fig. 3b), so that the PF_6^- peak can be used as internal standard. The cells presented in Fig. 3 are listed in Table II as Si-Li #1-3, with Si-Li #1 and Si-Li #3 being the cells with the least and the most number of cycles, respectively. Knowing N_{FEC} of these cells and applying the model developed in Fig. 6, $Q_{irr}^{drop\ (predicted)}$ was calculated and compared to the experimentally observed Q_{irr}^{exp}. The remaining FEC in the cells ($FEC_{left\ (EC)}$) was then calculated from the electrochemical data as:

$$FEC_{rem.\ (EC)} = 1 - \frac{Q_{irr}^{exp}}{Q_{irr}^{drop\ (predicted)}} \quad [2]$$

The resulting values for the remaining FEC obtained by Equation 2 were then compared to the NMR data for which the remaining FEC ($FEC_{rem.\ (NMR)}$) was obtained from the integral ratio of the FEC and PF_6^- peaks. As shown in Table II, both ways of determining the remaining amount of FEC result in essentially identical values for the cells in Fig. 3 (Si-Li #1-3), thereby validating the assumptions underlying the respective analyses, particularly the assumption that FEC is reduced exclusively and that therefore essentially all of the observed cumulative irreversible capacity goes into FEC reduction.

In order to understand the reductive decomposition of FEC in more detail, the cumulative irreversible capacity at the cycle where the rapid capacity drop initiates was converted into a total molar amount of electrons, n_e (in units of μmol) "consumed" in parasitic reactions involved in the continuous renewal of the SEI. This was done by converting the measured irreversible capacity into units of As and dividing it by the Faraday constant. Similarly, the specific amount of FEC was converted into a total molar amount of FEC, n_{FEC}, in the cells. Both n_e and n_{FEC} obtained for all cells for which a rapid capacity drop was observed are summarized in Table III. By dividing n_e through n_{FEC}, the parameter β is obtained, which is a measure for the apparent number of electrons consumed per FEC molecule. The $\beta_{apparent}$-values for all the tested cells vary around two, with an average value and standard deviation of $\beta_{apparent} = 1.9 \pm 0.3$. This could be interpreted to indicate that the reduction of FEC might follow a 2-electron mechanism. However, one has to be aware that the parasitic reactions on the lithium electrode in a silicon-lithium cell, i.e., with a virtually infinite amount of lithium, are not discernible in the irreversible capacity. Therefore, since it is likely that lithium will also decompose FEC, one needs to quantify the amount of decomposed FEC on the lithium counter electrode in order to determine its contribution to the FEC consumption in the Si-Li cells.

In order to answer the question of how much FEC is consumed on the lithium electrode, three Li-Li cells were prepared and cycled with the same current and over the same time like the Si-Li #1 cell (i.e., passing the same amount of total coulombs as during the cycling of the Si-Li #1 cell), also using 75 μL LP57 electrolyte with 5%$_{wt}$ FEC (Table II). Right after the Li-Li cells were cycled, ^{19}F-NMR spectra of the electrolytes were recorded. Since in this case two lithium electrodes are used, the amount of FEC decomposition on the two lithium electrodes should be exactly twice that which would be decomposed on the lithium electrode in the Si-Li #1 cell. Interestingly, the remaining FEC in the Li-Li cells was identical to that found for the Si-Li #1 cell, suggesting that ≈50% of the overall FEC consumption in a Si-Li cell is due to its reaction at the lithium counter electrode. Since the FEC consumption on lithium does not add to the cumulative irreversible capacity, this means that in fact only 50% of the FEC decomposition is accounted for in the cumulative irreversible capacity. This in turn means that the apparent 2-electron reduction of FEC in Si-Li cells (i.e., $\beta_{apparent} = 1.9 \pm 0.3$ obtained from Table III) is 2-fold lower than the actual number of electrons involved in the overall FEC reduction process, viz., $\beta_{actual} = 3.8 \pm 0.6$.

Scheme 1 (left panel) visualizes these processes on the silicon and the lithium electrode in a Si-Li cell, using an exemplary amount of four FEC molecules in the electrolyte and for simplicity assuming

Table III. Total moles of electrons, n_e, consumed in parasitic reactions and total moles of FEC, n_{FEC}, in the Si-Li cells for which a rapid capacity drop was observed (data shown in Figs. 1 and 2). The value of n_e was calculated from of the cumulative irreversible capacity up to the cycle where the rapid capacity drop initiated. The apparent number of electrons per consumed FEC, $\beta_{apparent}$, is defined as n_e/n_{FEC}.

Cell details	n_e [μmol]	n_{FEC} [μmol]	$\beta_{apparent}$
5% FEC, 75 μL	80.8	39.4	**2.05**
5% FEC, 75 μL	83.7	39.4	**2.12**
10% FEC, 75 μL	133.9	75.7	**1.77**
10% FEC, 75 μL	130.9	75.7	**1.73**
1% FEC, 150 μL	34.6	16.1	**2.16**
1% FEC, 150 μL	37.4	16.1	**2.33**
5% FEC, 150 μL	125.9	78.9	**1.60**
5% FEC, 150 μL	127.8	78.9	**1.62**

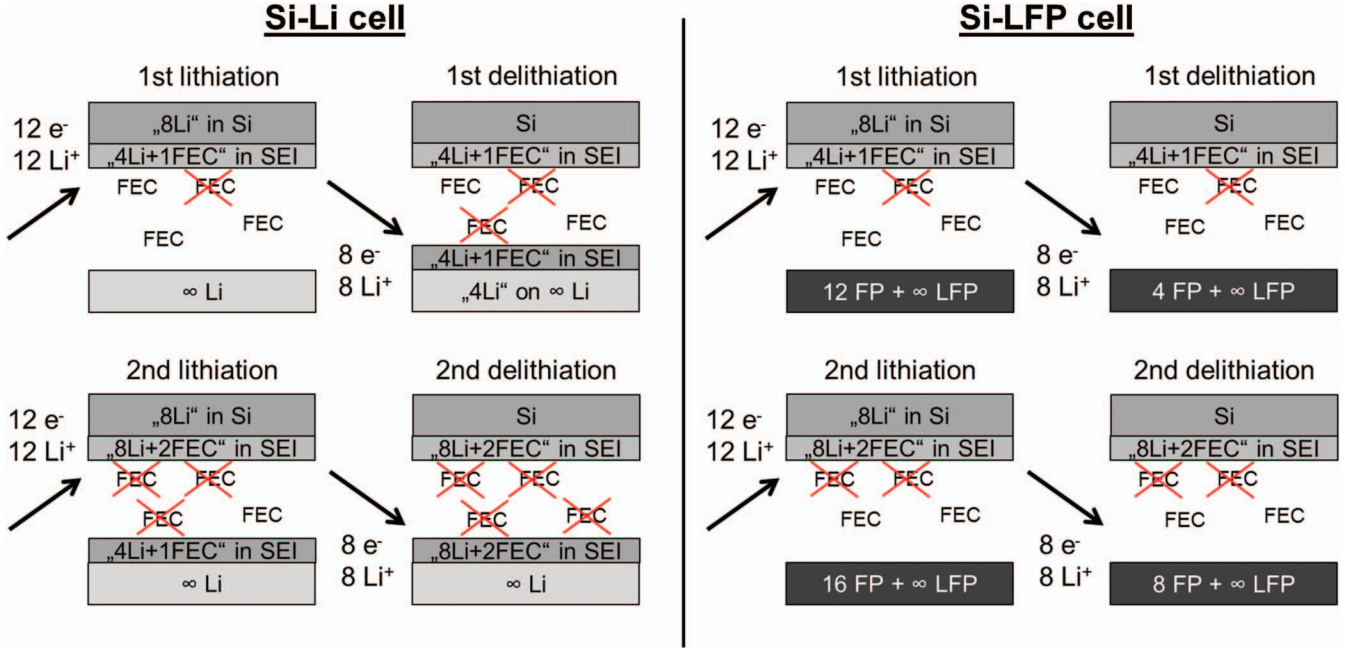

Scheme 1. Illustration of the FEC consumption in a Si-Li (left) and Si-LFP cell (right). The large excess of lithium in the lithium and the LFP counter electrodes compared to the capacity of the silicon electrodes is indicated by the ∞ sign.

that the reduction of FEC requires four electrons (i.e., $\beta_{actual} = 4$). If we then construct an example where 12 e^- and 12 Li^+ are transferred to the silicon electrode during the first lithiation cycle, then 8 ($e^- + Li^+$) could alloy with the silicon, while the remaining 4 ($e^- + Li^+$) could reduce one molecule of FEC ($\beta_{actual} = 4$) to build up the SEI. Since these four electrons are irreversibly consumed in the SEI formation, only 8 ($e^- + Li^+$) can be dealloyed from silicon during the first delithiation. From these 8 ($e^- + Li^+$) four go into the reduction of another FEC molecule on the lithium electrode and the other four are plated as lithium metal. As the lithium metal is an infinite reservoir of lithium, in the following cycle again 12 ($e^- + Li^+$) can be stripped from the lithium metal, starting the cycle over again. Summing up over each of the two cycles, the apparent irreversible capacity is four electrons and two molecules of FEC are reduced, giving a total of two electrons per consumed FEC or, in other words, $\beta_{apparent} = 2$.

In order to further prove that the total FEC decomposition in a Si-Li cell is split 50/50 between the silicon and the lithium electrode, the lithium counter electrode was replaced by an electrode on which no FEC decomposition would occur, namely with an LFP counter electrode. Under this premise, a Si-LFP cell was cycled with 75 µL LP57 electrolyte containing 2%$_{wt}$ FEC ($N_{FEC} = 14.80$ $\mu mol_{FEC}/mg_{electrode}$; see Si-LFP #1 in Table II); note that the FEC/$LiPF_6$ integral ratio determined by NMR for this 2%$_{wt}$ FEC electrolyte (=3.75) is 6% higher than predicted from the ratio obtained with the 5%$_{wt}$ FEC electrolyte (i.e., $2/5 \cdot 8.85 = 3.54$, Table II), which is due to pipetting errors when adding very small amounts of FEC. For Si-Li cells, the predicted cumulative irreversible capacity until the onset of the rapid capacity drop derived from the linear regression correlation of $Q_{irr}^{drop\ (projected)}$ vs. N_{FEC} (see caption of Fig. 6) would amount to 744 mAh/$g_{electrode}$, at which point all FEC should be consumed. Based on the above finding that 50% of the FEC is decomposed on the lithium counter electrode in Si-Li cells, the predicted cumulative irreversible capacity until the rapid capacity drop for Si-LFP cells would be 1488 mAh/$g_{electrode}$, since FEC is not decomposed on the LFP. Therefore, we stopped the cycling of the Si-LFP #1 cell once a cumulative irreversible capacity of 776 mAh/$g_{electrode}$ was reached (i.e., close to 744 mAh/$g_{electrode}$), at which point we would expect that ≈50% of the FEC would still remain in the cell. Indeed, as shown in Table II (last row), 47% FEC remain in the cell after a cumulative irreversible capacity of 776 mAh/$g_{electrode}$, providing further proof to the above finding that 50% of the FEC are consumed by the lithium electrode when cycling Si-Li cells. The number of electrons per FEC can now be determined from the cumulative irreversible capacity of the Si-LFP #1 cell (776 mAh/$g_{electrode}$ ≡ 29.0 $\mu mol_{electrons}/mg_{electrode}$) and the molar consumption of FEC (53% of 14.8 $\mu mol_{FEC}/mg_{electrode}$ amounting to 7.84 $\mu mol_{FEC}/mg_{electrode}$), yielding a value of $\beta_{actual} = 3.7$, essentially identical with the above derived value.

Additionally, a second Si-LFP cell (Si-LFP #2 in Table II) was tested replacing the two glass fiber separators by two conventionally used H2013 polyolefin separators (note that the FEC/$LiPF_6$ integral ratio of 3.29 of this freshly made 2%$_{wt}$ FEC containing electrolyte is 7% lower than what would be predicted based on the 5%$_{wt}$ electrolyte, which again (see above) is due to pipetting errors for very low FEC contents). Due to the lower pore volume of the polyolefin separators, the electrolyte volume was reduced to 30 µL. Assuming the above proposed four electron reduction of FEC the total FEC depletion is expected at a cumulative irreversible capacity of 752 mAh/$g_{electrode}$. As the cell was stopped at a cumulative irreversible capacity of 482 mAh/$g_{electrode}$, 36% of the added FEC is expected to remain in the cell. This is in excellent agreement with the subsequent quantification by ^{19}F-NMR, which reveals that 33% of the initial FEC is still present in the electrolyte. This clearly proves that the FEC consumption in the here presented experiments is not affected by the nature of the separator and indeed proceeds according to an overall four-electron reduction.

The processes in a Si-LFP cell with a capacity-wise largely oversized LFP counter electrode (Scheme 1, right panel) can again be illustrated using four molecules of FEC and $\beta_{actual} = 4$. During the first lithiation, as for the Si-Li case, 12 ($e^- + Li^+$) are transferred, with 8 ($e^- + Li^+$) alloying the silicon and 4 ($e^- + Li^+$) reducing one molecule of FEC (i.e., $\beta_{actual} = 4$). In the subsequent delithiation, 8 ($e^- + Li^+$) are removed from silicon. In contrast to the Si-Li case, all 8 ($e^- + Li^+$) are intercalated into FP and no further FEC molecule is decomposed. As the LFP is capacitively oversized, 12 ($e^- + Li^+$) can be deintercalated again in the following cycle. Summing up for each of the two cycles, the apparent irreversible capacity is again four electrons, but only one molecule of FEC is decomposed, giving a total of four electrons per consumed FEC. Thus, since the LFP electrode is an "inert" electrode, the irreversible capacity in a Si-LFP system shows

the real amount of four electrons necessary to reduce one molecule of FEC, i.e., $\beta_{apparent} = \beta_{actual}$.

Summarizing the above analysis, the continuous reduction of FEC on both lithium and silicon electrodes consumes close to four electrons per decomposed FEC molecule ($\beta_{actual} = 3.8 \pm 0.6$), which is substantially larger than in the most reduction mechanisms proposed in the literature.[22,26–28,30,31,36,46–49] A mechanism which would be consistent with this β-value will be presented below. Another important aspect of the FEC consumption analysis in Si-Li vs. Li-Li cells is that the FEC consumption per electrode during charge/discharge cycling only depends on the overall exchanged coulombs. Thus, the continuous parasitic electrolyte reduction with silicon anodes is not any different from that with metallic lithium anodes, at least when silicon is cycled between 10 mV and 1.2 V vs. Li/Li^+. This, unfortunately, suggests that silicon anodes may not have any hoped-for advantages in terms of continuous electrolyte consumption over metallic lithium anodes.

Gas analysis of Si-LFP cell by OEMS.—As presented before, three phases with different CO_2 evolution rates were observed in the OEMS measurement (Fig. 5b), which might be interpreted as: i) fast initial formation of an SEI monolayer on the electrode; ii) subsequent slower growth of a multi-layered SEI; and, iii) continuous formation of new SEI due to cracks caused by silicon volume expansion/contraction during lithiation/delithiation. In comparison, no hydrogen was evolved during the fast initial SEI formation phase and was only observed after a few hours into the charging process conducted at a rate of C/20. The hydrogen evolution rate, however, closely matches the CO_2 evolution rate in the third phase of the charging process (indicated by essentially parallel lines of concentration vs. time after ≈10 hours in Fig. 5b).

In the following, we will take a closer look at the first phase of the lithiation process, as it can provide information on the number of CO_2 molecules produced during the decomposition of an FEC molecule. After 4.2 minutes of the first-cycle lithiation at C/20 (≡ 148 μA/cm^2 or 262 μA), the CO_2 concentration in the OEMS accumulates to 460 ppm while the silicon electrode remains above ≈800 mV vs. Li/Li^+ (see Fig. 5a). At this potential, no intercalation into graphite nor into silicon is expected. Therefore, all current passed within these first 4.2 minutes will go into FEC reduction. The total amount of electrons during that period is n_e = 66 mAs = 684 nmol and the 460 ppm of CO_2 equate to a total of 178 nmol (based on an OEMS cell volume of 9.5 mL and 24.5 L/mol at 25°C/1 bar for an ideal gas). From this we can calculate the electrons per CO_2:

$$\frac{n_e}{n_{CO_2}} = \frac{684\ \text{nmol}}{178\ \text{nmol}} \approx 3.8\ \frac{e^-}{CO_2} \qquad [3]$$

Comparing the value of $e^-/CO_2 \approx 3.8$ with the above determined value of $e^-/FEC \approx 3.8 \pm 0.6$ (≡ β_{actual}), clearly indicates that the decomposition of one molecule of FEC produces one molecule of CO_2.

Next we will evaluate whether our above assumption of the formation of an SEI monolayer within the very initial phase of the lithiation process is reasonable. During this phase, CO_2 is evolved at a very high rate, producing 178 nmol within the first 4.2 minutes (see above). As determined in the Experimental section, the overall BET surface area of silicon, VGCF-H fibers, and the carbon fiber paper in the OEMS electrode equates to 0.017 m^2/cm$^2_{electrode}$ or to 0.030 m^2 per electrode. Since we have shown that each FEC molecule produces one CO_2 molecule during its decomposition and consumes ≈4 e^- (i.e., ≈4 Li^+), the grantedly most simple estimate would be that the decomposition product should be composed of 11 atoms (10 atoms/FEC - 3 atoms/CO_2 + 4 Li atoms). Assuming that every atom occupies a square with a side length equal to a carbon-carbon single bond length of 0.15 nm,[45] the area covered by one FEC decomposition product would be 11 × (0.15 nm)^2 = 0.25 nm^2. Consequently, the total area covered by 178 nmol of decomposition products can be estimated to be roughly 178 nmol × 0.25 nm^2 × N_A = 0.027 m^2 ($N_A = 6.023 \cdot 10^{23}$ atoms/mol). This estimated monolayer area very well matches the total surface area of the electrode (0.030 m^2), providing strong evidence that the high CO_2 evolution rate in the initial part of the first-cycle lithiation is due to an SEI monolayer formation on the electrode.

Reductive decomposition mechanism of fluoroethylene carbonate.—In the literature, a large variety of reduction mechanisms for FEC have been proposed.[22,26–28,30,31,36,46–49] However, there is neither a consensus on the reduction products nor on the number of electrons which are transferred to FEC and its decomposition products. For example, Wang et al. proposed a 1-electron reduction of the FEC molecule leading to a ring opening and followed by a dimerization to a dicarbonate.[31] Similar to this mechanism, Chen et al. proposed the ring opening in a 1-electron mechanism followed by a dimerization or, as an alternative pathway, a defluorination resulting in LiF and $(CH_2CHOCO_2Li)_n$.[47] Etacheri et al. proposed the transformation of FEC to vinylene carbonate (VC) by HF elimination with subsequent formation of LiF and reduction of the formed double bond, initiating the polymerization to poly(VC).[22] This was revised in a later publication by the same group, with Markevich et al. proposing a mechanism leading to the release of CO_2 aside with a variety of further decomposition products like H_2, LiF, Li_2CO_3 and a polymeric compound.[46] Nakai et al. proposed a 3-electron mechanism yielding LiF, Li_2CO_3, H_2 and a polymer.[30]

Even numerous, partially contradicting mechanisms have been proposed, there is a common finding. In particular, LiF was observed or proposed independently by several authors,[22,26–28,30,36,46–49] whereby the study by Schroder et al. indicates that the LiF content of the SEI is higher in the presence of FEC.[36] Formation of LiF also is consistent with our observations since we did not see any soluble fluorine containing decomposition products in the electrolyte by ^{19}F-NMR, even though we cannot exclude the formation of other fluoride containing solids. In recent publications by Balbuena and co-workers, applying ab initio modeling, the 1-electron reduction of FEC was suggested to yield an FEC-radical anion, decomposing into CO_2, F^-, and a vinoxyl-radical.[27,28] The formation of the vinoxyl-radical was also detected experimentally by Shkrob et al. by means of EPR experiments.[49] The release of CO_2 accompanied with the formation of LiF and the vinoxyl-radical is further supported by our observation that per FEC molecule also one molecule of CO_2 is released.

Based on the literature and our measurements, our proposed mechanism (Scheme 2) also starts with an initial electron transfer to the carbonyl carbon (1st electron transfer), which due to its bond to three oxygens is the most positively charged atom of the FEC molecule. Subsequently, the ring of the radical anion is opened, followed by the elimination of CO_2 and fluoride, which forms LiF with lithium ions in the electrolyte. It is quite reasonable to assume that the possibility to eliminate fluoride ions is the reason why the structurally similar molecules FEC and EC lead to very different decomposition products, resulting in significantly different structures of the respective SEIs. After fluoride and CO_2 elimination, the vinoxyl-radical remains, which is stabilized via the carbon-oxygen double bond. The formation of CO can be ruled out by our OEMS measurement, contradicting some theoretical calculations in literature where release of CO was proposed to lead to alternative pathways which do not produce the vinoxyl-radical.[27,28] Since we found the release of one CO_2 per FEC molecule, we believe that the pathway leading to the vinoxyl-radical, CO_2, and LiF is at least the most predominant one. Neither in the paper by Shkrob et al.[49] nor in the papers by the group of Balbuena[27,28] further electron transfer to the vinoxyl-radical was considered, as there was no information on the total number of electrons involved in the reduction of FEC, even though it was pointed out by Leung et al. that further electron transfer cannot be ruled out.[28] Our results, however, clearly show that a total of four electrons are consumed in the reductive decomposition of FEC. Therefore, the vinoxyl-radical has to be further reduced (2nd electron transfer), which should easily be possible considering its structure with a carbon-oxygen double bond, resulting in lithium-ethenolate (see second line in Scheme 2).

Lithium-ethenolate can be further reduced (3rd electron transfer) to lithium oxide and an ethenyl-radical (see second line in Scheme 2). We believe that the driving force for this reaction is the formation of the

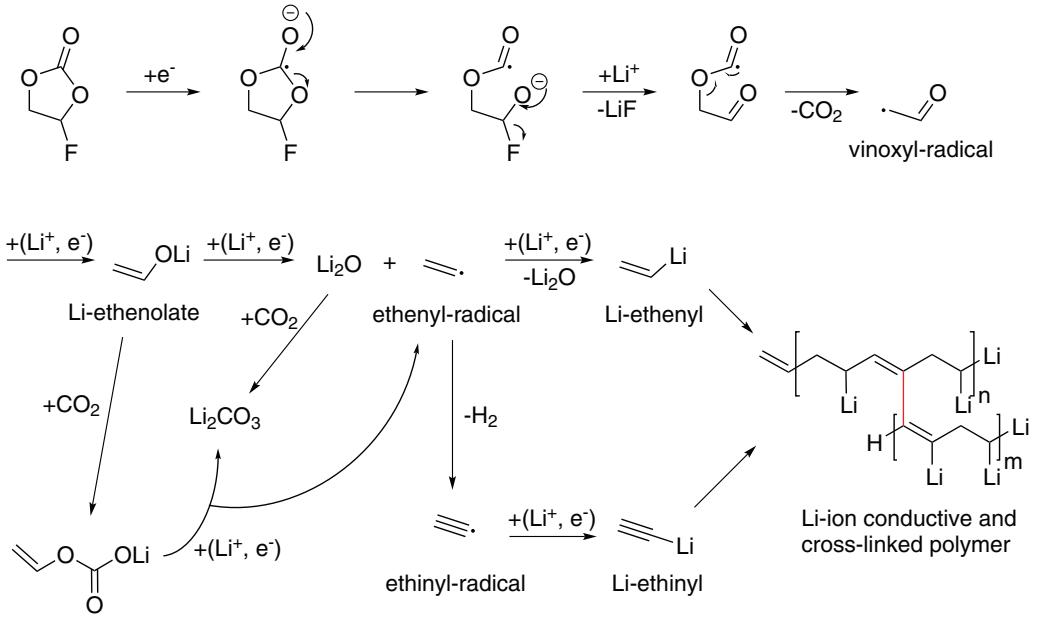

Scheme 2. Proposed mechanism for the reductive decomposition of fluoroethylene carbonate (FEC), with an overall consumption of four electrons per FEC molecule, leading to CO_2, LiF, Li_2O, H_2, Li_2CO_3, and a partially cross-linked polymer.

stable Li_2O, which was found as part of the SEI by XPS measurements of a cycled silicon anode if FEC was present in EC/DEC electrolyte.[36] An alternative 3rd electron transfer step leading to the same ethenyl-radical, is the chemical reaction of lithium-ethenolate with CO_2 to an alkylcarbonate, which can then be reduced to the ethenyl-radical and Li_2CO_3 (see third line in Scheme 2). The latter is reported as SEI component in the literature, but different formation mechanisms were proposed.[30,46] Li_2CO_3 could also be formed by the reaction of Li_2O with CO_2, which might also explain why it was not considered an energetically feasible FEC reduction product in the calculations by Leung et al.[28]

Even though we currently have no experimental evidence for it, we believe that in accordance with the reports by Shkrob et al.[49] and Markevich et al.[46] a cross-linked[49] and oxygen-poor[46] polymer is formed. Therefore we assume that further direct reduction of the reactive ethenyl-radical (4th electron transfer) yields lithium-ethenyl. Alternatively, the ethenyl-radical could first be stabilized by release of hydrogen, yielding an ethinyl-radical, which is then further reduced to lithium-ethinyl. The latter pathway would be consistent with the observation that the CO_2 and the H_2 evolution rate are very similar in the latter stages of the first lithiation cycle (see Fig. 5b).

Both lithium-ethenyl and lithium-ethinyl would likely polymerize, yielding a partially cross-linked polymer, which might be lithium ion conductive due to the weak carbon-lithium bond. This property might give the SEI the desired property of an electron insulating but lithium ion conductive layer, and might explain why the observed impedances in electrolytes with FEC are lower compared to the ones in FEC-free electrolytes after extended cycling;[22,26,36,49] the initially higher impedance with FEC containing electrolytes can be explained by the initially faster SEI formation with FEC.[36] In addition, the cross-linking renders the polymer elastomeric, which might enable it to better withstand the stresses caused by the volumetric expansion/contraction of silicon particles during lithiation/delithiation, reducing the extent of SEI rupture.

Implications for commercial silicon cells.—From the above analysis, it is clear that FEC is able to extend the cycle-life of silicon anodes until it is consumed, so that the cumulative irreversible capacity until the rapid capacity drop occurs is simply related to the specific amount of FEC, described by the added $\mu mol_{FEC}/mg_{electrode}$. In the following, we will replace the cumulative irreversible capacity by the number of cycles until the rapid capacity drop to give a rough estimate on how long FEC can stabilize the performance in commercial cells with realistic electrolyte/active material ratios. Note that the transformation from the universally applicable cumulative irreversible capacity to the number of cycles in this calculation is only valid for the silicon electrodes and cycling conditions used in this work, as other systems with different silicon morphology, particle size, or less volume expansion achieved by limiting the silicon capacity will definitely influence the irreversible capacity loss per cycle. Figs. 1 and 2 show that the rapid capacity drop is not observed within 450 charge/discharge cycles for $20\%_{wt}$ FEC and 75 µL of electrolyte ($\equiv 43.5\ \mu mol_{FEC}/mg_{electrode}$; see green line in Fig. 1) and for $\geq 10\%_{wt}$ FEC and 150 µL of electrolyte (i.e., for $\geq 56.1\ \mu mol_{FEC}/mg_{electrode}$; see magenta line in Fig. 2). This is consistent with the literature, which shows that the use of FEC as co-solvent (typically $\geq 10\%_{wt}$ FEC) strongly stabilizes the cycle-life of silicon anodes.[22,25,46] The cycle number of the Si-Li cells at which the rapid capacity drop occurs is depicted by the black symbols in Fig. 7 (data from Figs. 1 and 2). Since the cumulative irreversible capacity at the rapid capacity drop, Q_{irr}^{drop}, is the intrinsic physical-chemical parameter that correlates with N_{FEC} (see Fig. 6), the correlation between cycle number at the rapid capacity drop with N_{FEC} is less stringent due to the fact that the coulombic efficiencies of the different cells are not perfectly identical. Nevertheless, the x-axis intercept of the linear regression line in Fig. 7 (black line) which represents the consumption of FEC during the first cycle ($3.3\ \mu mol_{FEC}/mg_{electrode}$), is reasonably close to the more precise value obtained in Fig. 6 ($4.1\ \mu mol_{FEC}/mg_{electrode}$). Therefore, while not being exactly correct, the black regression line in Fig. 7 can provide a rough estimate for the numbers of cycles until the rapid capacity drop will occur for a given specific amount of FEC in Si-Li cells. To be more generally applicable to any type of silicon anode, the specific amount of FEC should be referenced to the mass of silicon (N_{FEC}^{Si} in $\mu mol_{FEC}/mg_{Si}$), as was explained in the discussion of Fig. 6.

Since we found that 50% of the FEC in Si-Li cells is consumed at the lithium electrode, the correlation between the number of cycles until the rapid capacity drop and N_{FEC}^{Si} must be corrected for this effect in the case of Si full-cells. This is given by the red line in Fig. 7, where it is assumed that the potential of the Si full-cell cathode is sufficiently low to not oxidize FEC (i.e., the x-axis intercept is half of its value for the black line and the slope is doubled). In analogy, also the model obtained in Fig. 6 can be modified analogously to

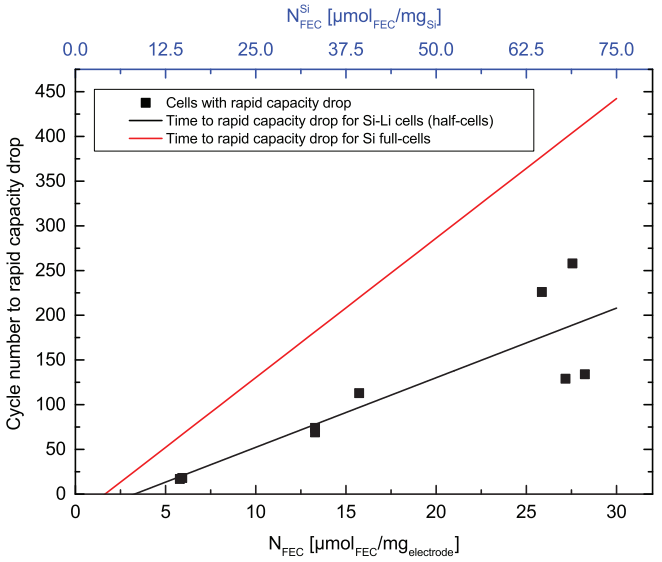

Figure 7. Cycle number at which the rapid capacity drop is observed or expected vs. specific amount of FEC in the cell (N_{FEC}) based on the data in Figs. 1 and 2 and on the Si-Li #3 cell in Fig. 3. The black line is a least-squares regression line through the data obtained for these 9 cells: cycle#$_{drop}$ = 7.8 ($\mu mol_{FEC}/mg_{electrode}$)$^{-1}$ × N_{FEC} – 25.5, with an x-axis intercept of 3.3 $\mu mol_{FEC}/mg_{electrode}$. The red line is the predicted cycle life for Si full-cells with cathodes at sufficiently low potential to not oxidize FEC: cycle#$_{drop}$ = 15.6 ($\mu mol_{FEC}/mg_{electrode}$)$^{-1}$ × N_{FEC} – 25.7, with an x-axis intercept of 1.65 $\mu mol_{FEC}/mg_{electrode}$. The top x-axis displays the amount of FEC normalized to the mass of silicon.

account for Si full-cells. In other words, by simply summing up the irreversible capacities, one can predict how much FEC is left in the cell and at which value of the cumulative irreversible capacity it will be entirely consumed.

With regards to the expected impact of FEC co-solvent in real batteries, one has to consider the fact that the amount of electrolyte used in coin cell testing typically ranges from ≈50–200 µL/cm^2, (e.g., 75 and 150 µL of added electrolyte in Fig. 1 corresponds to 95 and 190 µL/cm^2). On the other hand, the amount of added electrolyte in real batteries is only slightly above the value corresponding to the void volume in the electrodes (≈35%) and the separator (≈50%), which results in an electrolyte/anode/cathode mass fraction of ≈20/25/55 (not counting the current collectors).[50] For a battery with 2 mAh/cm^2 areal capacity using active materials with anode/cathode specific capacities of ≈360/≈150 mAh/g (e.g., graphite/NMC) at an active material content of 90%$_{wt}$, the electrode areal weights (anode and cathode without current collector) would amount to ≈21 mg/cm^2, which would require the addition ≈5 µL/cm^2 of electrolyte (using the above given weight fraction and assuming a density of ≈1 g/cm^3). Thus, the amount of electrolyte volume per area in a real typical battery is ≈10–40 times lower than what is used in typical coin cell testing. Based on these considerations, we can now estimate the $\mu mol_{FEC}/mg_{electrode}$ which would be available in a real battery using 20%$_{wt}$ FEC as co-solvent and assuming that also 5 µL/cm^2 electrolyte (corresponding to ≈9.4 $\mu mol_{FEC}/cm^2$) would be added to a battery with 2 mAh/cm^2 areal capacity. If one were to achieve the theoretical specific capacity of 1440 mAh/$g_{electrode}$ for our 40%$_{wt}$ Si electrodes, the required areal weight of the silicon electrode would be ≈1.4 $mg_{electrode}/cm^2$, resulting in a specific FEC amount of ≈6.8 $\mu mol_{FEC}/mg_{electrode}$. A comparison with Fig. 7 shows, that the specific amount of FEC estimated to be present in a real battery with 20%$_{wt}$ FEC co-solvent would only stabilize the silicon anode performance for roughly 75 cycles (red line in Fig. 7). We believe that this is the explanation for frequently reported long cycle life of cells with silicon anodes and FEC co-solvent if tested in coin cells (>hundreds of cycles),[25,46] while to our knowledge this has never been reported for actual batteries, in which the amount of electrolyte in terms of µL/cm^2 is much smaller.

Conclusions

This work focused on a fundamental understanding of the effect of fluoroethylene carbonate (FEC) on the SEI formation on silicon-carbon composite electrodes. Consistent with the literature, it was found that the cyclability of cells is significantly improved when FEC is used as electrolyte additive. However, these cells experienced a sudden failure with a rapid capacity drop, depending on the specific amount of FEC in the cells (in units of $\mu mol_{FEC}/mg_{electrode}$). It was shown by ^{19}F-NMR spectroscopy that this rapid capacity drop occurs once all of the added FEC has been consumed, at which point the polarization of the silicon-carbon composite electrode increases as evidenced by charge/discharge experiments with a lithium reference electrode. By the use of On-line Electrochemical Mass Spectrometry (OEMS) it was proven that in the presence of FEC the reduction of other electrolyte components is prevented, i.e. FEC gets reduced almost exclusively. Therefore, the cumulative irreversible capacity until the rapid capacity drop is linearly related to the specific amount of FEC (in units of $\mu mol_{FEC}/mg_{electrode}$) in the cell. The quantification of the FEC consumption by ^{19}F-NMR is further proposed as a new method to study the continuous electrolyte reduction during cycling of cells with silicon anodes.

A comparison of the FEC consumption of Si-Li half-cells with that in Li-Li as well as Si-LFP cells revealed that ≈50% of the FEC in Si-Li half-cells is consumed by the Li-electrode. This in turn means that the electrolyte consumption of Si-anodes if cycled between 10 mV and 1.2 V vs. Li/Li$^+$ is identical to that of metallic lithium anodes, and only dependent on the total amount of charge passed in the respective charge/discharge cycles. Finally, based on the correlation between the cumulative irreversible capacity and the specific amount of FEC in the cell it was shown that the reductive decomposition of one FEC molecule consumes four electrons. Additionally, by quantification of the evolved gases in the cell using OEMS it was found that one molecule of CO_2 is released for every molecule of FEC that is reduced. Combining our results with previous findings in literature, a new mechanism for the reductive decomposition of FEC was proposed yielding CO_2, LiF, Li_2O, Li_2CO_3, H_2 and a partially cross-linked polymer.

Acknowledgment

The authors thank BMW for financial support. S. S. and M. M. gratefully acknowledge funding by BASF SE through its electrochemistry and battery research network. We thank Jeff Dahn (University of Dalhousie) for very fruitful discussions. Many thanks also go to Uta Schwenke and Morten Wetjen from our group for helpful advices and great contributions to this work.

Note added in proof.—After submission of our manuscript for review, an article appeared by R. Petibon et al.,[51] who observed the same phenomenon of a rapid capacity drop after the consumption of FEC in 200 mAh pouch cells with $LiCoO_2$ cathodes and Si-alloy/graphite composite anodes. The similarity of their results and ours clearly point out that the continuous electrolyte consumption is a severe problem for silicon-based electrodes and that the electrolyte to active material ratio always has to be considered when Si-electrodes are used.

References

1. M. T. McDowell, S. W. Lee, W. D. Nix, and Y. Cui, *Adv. Mater. (Weinheim, Ger.)*, **25**, 4966 (2013).
2. O. Groeger, H. A. Gasteiger, and J.-P. Suchsland, *J. Electrochem. Soc.*, **162**, A2605 (2015).
3. USABC http://www.uscar.org/guest/article_view.php?articles_id=85, accessed on 02/19/2016.
4. D. Andre, S.-J. Kim, P. Lamp, S. F. Lux, F. Maglia, O. Paschos, and B. Stiaszny, *J. Mater. Chem. A*, **3**, 6709 (2015).

5. U. Kasavajjula, C. Wang, and A. J. Appleby, *J. Power Sources*, **163**, 1003 (2007).
6. L. Lu, X. Han, J. Li, J. Hua, and M. Ouyang, *J. Power Sources*, **226**, 272 (2013).
7. M. N. Obrovac and L. Christensen, *Electrochem. Solid-State Lett.*, **7**, A93 (2004).
8. D. Larcher, S. Beattie, M. Morcrette, K. Edstroem, J.-C. Jumas, and J.-M. Tarascon, *J. Mater. Chem.*, **17**, 3759 (2007).
9. P. Limthongkul, Y.-I. Jang, N. J. Dudney, and Y.-M. Chiang, *Acta Mater.*, **51**, 1103 (2003).
10. W.-J. Zhang, *J. Power Sources*, **196**, 13 (2011).
11. L. Y. Beaulieu, K. W. Eberman, R. L. Turner, L. J. Krause, and J. R. Dahn, *Electrochem. Solid-State Lett.*, **4**, A137 (2001).
12. C. K. Chan, H. Peng, G. Liu, K. McIlwrath, X. F. Zhang, R. A. Huggins, and Y. Cui, *Nat Nano*, **3**, 31 (2008).
13. H. Kim, B. Han, J. Choo, and J. Cho, *Angew. Chem., Int. Ed.*, **47**, 10151 (2008).
14. N. Liu, H. Wu, M. T. McDowell, Y. Yao, C. Wang, and Y. Cui, *Nano Lett.*, **12**, 3315 (2012).
15. R. A. Huggins and W. D. Nix, *Ionics*, **6**, 57 (2000).
16. X. H. Liu, L. Zhong, S. Huang, S. X. Mao, T. Zhu, and J. Y. Huang, *ACS Nano*, **6**, 1522 (2012).
17. A. Magasinski, P. Dixon, B. Hertzberg, A. Kvit, J. Ayala, and G. Yushin, *Nat Mater*, **9**, 353 (2010).
18. K. Evanoff, J. Khan, A. A. Balandin, A. Magasinski, W. J. Ready, T. F. Fuller, and G. Yushin, *Adv. Mater. (Weinheim, Ger.)*, **24**, 533 (2012).
19. H. Li, X. Huang, L. Chen, Z. Wu, and Y. Liang, *Electrochem. Solid-State Lett.*, **2**, 547 (1999).
20. J. Christensen and J. Newman, *J. Electrochem. Soc.*, **151**, A1977 (2004).
21. J. Christensen and J. Newman, *J. Electrochem. Soc.*, **152**, A818 (2005).
22. V. Etacheri, O. Haik, Y. Goffer, G. A. Roberts, I. C. Stefan, R. Fasching, and D. Aurbach, *Langmuir*, **28**, 965 (2012).
23. N.-S. Choi, K. H. Yew, K. Y. Lee, M. Sung, H. Kim, and S.-S. Kim, *J. Power Sources*, **161**, 1254 (2006).
24. E. Markevich, G. Salitra, K. Fridman, R. Sharabi, G. Gershinsky, A. Garsuch, G. Semrau, M. A. Schmidt, and D. Aurbach, *Langmuir*, **30**, 7414 (2014).
25. Y.-M. Lin, K. C. Klavetter, P. R. Abel, N. C. Davy, J. L. Snider, A. Heller, and C. B. Mullins, *Chem. Commun. (Cambridge, U. K.)*, **48**, 7268 (2012).
26. C. Xu, F. Lindgren, B. Philippe, M. Gorgoi, F. Bjoerefors, K. Edstroem, and T. Gustafsson, *Chem. Mater.*, **27**, 2591 (2015).
27. J. M. Martinez de la Hoz and P. B. Balbuena, *Phys. Chem. Chem. Phys.*, **16**, 17091 (2014).
28. K. Leung, S. B. Rempe, M. E. Foster, Y. Ma, J. M. Martinez del la Hoz, N. Sai, and P. B. Balbuena, *J. Electrochem. Soc.*, **161**, A213 (2014).
29. Y. Ma and P. B. Balbuena, *J. Electrochem. Soc.*, **161**, E3097 (2014).
30. H. Nakai, T. Kubota, A. Kita, and A. Kawashima, *J. Electrochem. Soc.*, **158**, A798 (2011).
31. Z. Wang, J. Xu, W.-H. Yao, Y.-W. Yao, and Y. Yang, *ECS Trans.*, **41**, 29 (2012).
32. V. L. Chevrier, L. Liu, D. B. Le, J. Lund, B. Molla, K. Reimer, L. J. Krause, L. D. Jensen, E. Figgemeier, and K. W. Eberman, *J. Electrochem. Soc.*, **161**, A783 (2014).
33. M. Metzger, J. Sicklinger, D. Haering, C. Kavakli, C. Stinner, C. Marino, and H. A. Gasteiger, *J. Electrochem. Soc.*, **162**, A1227 (2015).
34. N. Tsiouvaras, S. Meini, I. Buchberger, and H. A. Gasteiger, *J. Electrochem. Soc.*, **160**, A471 (2013).
35. B. Key, R. Bhattacharyya, M. Morcrette, V. Seznec, J.-M. Tarascon, and C. P. Grey, *J. Am. Chem. Soc.*, **131**, 9239 (2009).
36. K. Schroder, J. Alvarado, T. A. Yersak, J. Li, N. Dudney, L. J. Webb, Y. S. Meng, and K. J. Stevenson, *Chem. Mater.*, **27**, 5531 (2015).
37. S. P. Kuksenko and I. O. Konovalenko, *Russ. J. Appl. Chem.+*, **84**, 1179 (2011).
38. B. Zhang, M. Metzger, S. Solchenbach, M. Payne, S. Meini, H. Gasteiger, A. Garsuch, and B. L. Lucht *J. Phys. Chem. C*, **119**, 11337 (2015).
39. M. Nie, D. Chalasani, D. P. Abraham, Y. Chen, A. Bose, and B. L. J. Lucht *Phys. Chem. C*, **117**, 1257 (2013).
40. D. Aurbach, Y. Gofer, M. Ben-Zion, and P. J. Aped, *Electroanal. Chem.*, **339**, 451 (1992).
41. M. E. Spahr, T. Palladino, H. Wilhelm, A. Wuersig, D. Goers, H. Buqa, M. Holzapfel, and P. J. Novak, *Electrochem. Soc.*, **151**, A1383 (2004).
42. M. Winter and P. J. Novak, *Electrochem. Soc.*, **145**, L27 (1998).
43. M. Metzger, B. Strehle, S. Solchenbach, and H. A. Gasteiger, *J. Electrochem. Soc.*, **163**, A798 (2016).
44. S. F. Lux, I. T. Lucas, E. Pollak, S. Passerini, M. Winter, and R. Kostecki, *Electrochem. Commun.*, **14**, 47 (2012).
45. D. R. Lide, *Tetrahedron*, **17**, 125 (1962).
46. E. Markevich, K. Fridman, R. Sharabi, R. Elazari, G. Salitra, H. E. Gottlieb, G. Gershinsky, A. Garsuch, G. Semrau, M. A. Schmidt, and D. J. Aurbach, *Electrochem. Soc.*, **160**, A1824 (2013).
47. X. Chen, X. Li, D. Mei, J. Feng, M. Y. Hu, J. Hu, M. Engelhard, J. Zheng, W. Xu, J. Xiao, J. Liu, and J.-G. Zhang, *ChemSusChem*, **7**, 549 (2014).
48. M. Nie, D. P. Abraham, Y. Chen, A. Bose, and B. L. J. Lucht, *Phys. Chem. C*, **117**, 13403 (2013).
49. I. A. Shkrob, J. F. Wishart, and D. P. Abraham, *J. Phys. Chem. C*, **119**, 14954 (2015).
50. F. T. Wagner, B. Lakshmanan, and M. F. J. Mathias, *Phys. Chem. Lett.*, **1**, 2204 (2010).
51. R. Petibon, V. L. Chevrier, C. P. Aiken, D. S. Hall, S. R. Hyatt, R. Shunmugasundaram, and J. R. Dahn, *J. Electrochem. Soc.*, **163**, A1146 (2016).